

Original Research Article

Slight phenotypic variation in predators and prey causes complex predator-prey oscillations

Michael Bengfort^{a,1}, Ellen van Velzen^{b,*}, Ursula Gaedke^b^a Institute of Environmental Systems Research, School of Mathematics/Computer Science, Osnabrück University, Barbarastr. 12, 49069 Osnabrück, Germany^b University of Potsdam, Dept. Ecology and Ecosystem Modelling, Maulbeerallee 2, 14469 Potsdam, Germany

ARTICLE INFO

Article history:

Received 8 February 2017

Received in revised form 30 May 2017

Accepted 1 June 2017

Available online xxx

Keywords:

Predator-prey cycles

Phase relationships

Intermittent cycles

Adaptive traits

Eco-evolutionary dynamics

Complex dynamics

ABSTRACT

Predator-prey oscillations are expected to show a 1/4-phase lag between predator and prey. However, observed dynamics of natural or experimental predator-prey systems are often more complex. A striking but hardly studied example are sudden interruptions of classic 1/4-lag cycles with periods of antiphase oscillations, or periods without any regular predator-prey oscillations. These interruptions occur for a limited time before the system reverts to regular 1/4-lag oscillations, thus yielding intermittent cycles. Reasons for this behaviour are often difficult to reveal in experimental systems. Here we test the hypothesis that such complex dynamical behaviour may result from minor trait variation and trait adaptation in both the prey and predator, causing recurrent small changes in attack rates that may be hard to capture by empirical measurements. Using a model structure where the degree of trait variation in the predator can be explicitly controlled, we show that a very limited amount of adaptation resulting in 10–15% temporal variation in attack rates is already sufficient to generate these intermittent dynamics. Such minor variation may be present in experimental predator-prey systems, and may explain disruptions in regular 1/4-lag oscillations.

© 2017 Elsevier B.V. All rights reserved.

1. Introduction

The classical predator-prey models (Lotka, 1925; Volterra, 1928; Rosenzweig and MacArthur, 1963; Truscott and Brindley, 1994) predict oscillations with a 1/4-period lag between predator and prey (Bulmer, 1976). Such oscillations in species abundances have successfully been observed in empirical predator-prey systems (Gause et al., 1936; Elton and Nicholson, 1942; Utida, 1957; Huffaker, 1958; Luckinbill, 1974; McCauley et al., 1999; Ellner et al., 2001; Gilg et al., 2003). When systematic deviations from the classic 1/4-lag pattern are found, this gives a strong indication that there are important processes in the system that are not captured by a simple one-prey one-predator model. As a famous example, antiphase cycles (Yoshida et al., 2003; Becks et al., 2010) have a predator lag of 1/2 of the period instead of 1/4, and this is generally understood to be the result of rapid evolutionary change in the prey: in response to changes in grazing pressure, slower-growing

but grazing-resistant prey alternate in dominance with fast-growing but highly edible prey.

In some chemostat experiments more complex dynamics were observed: regular classic 1/4-lag oscillations were interrupted by time periods of antiphase cycles, or without any clear predator-prey cycles at all, before returning to 1/4-lag oscillations (Fig. 1; B. Blasius and G. Weithoff, pers. comm.). These *intermittent cycles* are not predicted by classic predator-prey models, or by models with prey evolution alone, and the reasons for this behaviour are generally unclear. The presence of regular 1/4-lag cycles before the interruptions indicates that these are not transient dynamics; moreover, chaotic dynamics are not possible in a simple predator-prey chemostat system because the nutrient-predator-prey system can be reduced to two dimensions (Jones and Ellner, 2007). Given the strictly controlled conditions in chemostats, it seems unlikely that intermittent cycles are an effect of environmental noise, raising the possibility of some unknown intrinsic mechanism in the system which leads to the observed complex dynamics.

Some previous models have shown dynamical behaviour with strong fluctuations in the amplitude of oscillations: these include models with two predators and two prey (Abrams and Shen, 1989; Mougi and Nishimura, 2007) and models with co-adaptation between predators and prey (Tirok et al., 2011; Mougi, 2012). The commonality in these models is the presence of trait variation or

* Corresponding author.

E-mail addresses: michael.bengfort@hzg.de (M. Bengfort), ellen.v.velzen.2@gmail.com (E. van Velzen).¹ Current address: Institute of Coastal Research, Helmholtz-Zentrum Geesthacht, Max-Planck-Straße 1, 21502 Geesthacht, Germany.

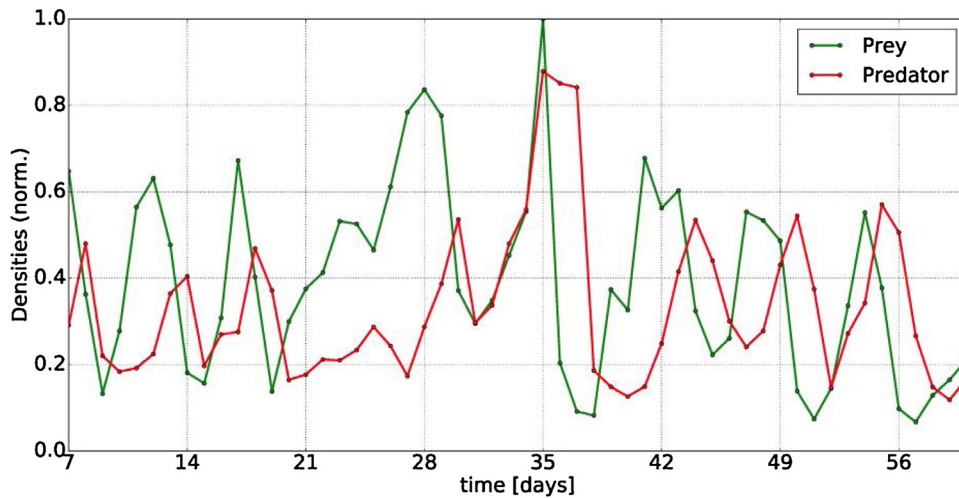


Fig. 1. Example of predator and prey densities over time in a flow-through chemostat experiment with an algal prey (green algae: *Monoraphidium minutum*) and small asexually reproducing metazoan herbivores (rotifers, started with one clone of *Brachionus calyciflorus*) as predators. Densities are normalized to the highest observed prey and predator densities, respectively (note that the highest predator density occurred outside of the window shown here). Day 7–20: classic 1/4-lag oscillations; approximately day 21–28: interruption of the 1/4-lag pattern by a period of near stasis for the predator, with no discernible phase relationship; day 29–60: return to 1/4-lag cycles (*pers. comm.* B. Blasius, G. Weithoff).

adaptation in both predators and prey, giving an indication of where to look for a possible explanation of the empirically observed intermittent cycles. However, in these models the potential differences in functional traits and the magnitude of trait changes are large: for example, in Tirok et al. (2011) prey edibility ranges from almost completely edible to almost completely inedible, and in Mougi (2012) the difference between highest and lowest attack rate is well over an order of magnitude. This stands in contrast with the highly controlled nature of the chemostat experiments under consideration, where intraspecific variation in both predators and prey are much less pronounced. Another potential mechanism for intermittent cycles is the evolution of phenotypic plasticity (Yamamichi et al., 2011), where alternation between 1/4-lag cycles and stationary dynamics is generated by temporal changes in the dominance of phenotypically plastic and non-plastic prey. But again there is no indication that such an extent of phenotypic plasticity is present in the algal prey for which intermittent cycles were observed.

We propose here that intermittent cycles may be the result of trait variation in the predators, combined with adaptation in the prey, which are too minor to be detected by routine measurements in empirical predator-prey systems. To test this hypothesis, we developed a new predator-prey model: we divided the predators into two groups (predator clones or phenotypes) which have distinct but overlapping prey spectra. Slight adaptation in the prey can make them less or more edible to each predator type (see Fig. 2). This model setup allows us to strictly control the amount of trait variation and adaptation present in the predators, enabling us to evaluate and predict the minimum amount of adaptation that can generate intermittent cycles.

2. Methods

2.1. Trait-based approach with two different predators

The idea behind the following model is that the predators are divided into two slightly different groups, and that the prey can adjust its edibility to both predators. Here, we assume that defence is bidirectional or incompatible (Abrams, 2000; Ellner and Becks, 2011) meaning that being better defended against one predator increases vulnerability to the other. This is generally applicable to size-specific predation. As one predator becomes more abundant,

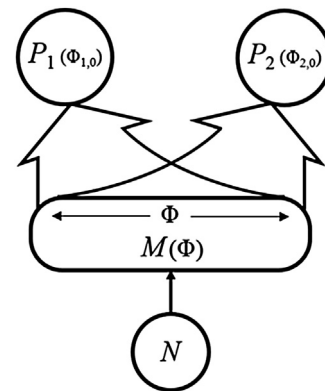


Fig. 2. Model concept: A single prey M with a defence trait Φ is consumed by two predators P_1 and P_2 . Both predators share the entire range of Φ they can consume, but have different values for the optimal value of Φ . The prey takes up the nutrients N .

the prey defence trait will shift to favour the other; because of this interplay, the predators can alternately dominate the system. Hiltunen et al. (2014a) called this dynamical behaviour a “predators taking turns” pattern. Because the presence of prey adaptation ensures that the each predator will become favoured when its density becomes low, this results in long-term coexistence of the two predators. This alternation in the dominance of the predator types can cause different dynamical behaviours of the system as a whole.

The model is based on a standard model for predator-prey systems in chemostats, which has recently provided a productive venue for the integration of theory and data (Fussmann et al., 2000, 2003, 2005; Jones and Ellner, 2007). The dynamics of nutrients, prey and predators are described by the following equations:

$$\frac{dN}{dt} = \delta(N_0 - N) - r \frac{NM}{K_M + N} \quad (1)$$

$$\frac{dM}{dt} = \left(\frac{rN}{K_M + N} - \frac{a_1(\Phi)P_1}{1 + a_1(\Phi)hM} - \frac{a_2(\Phi)P_2 \cdot f(M)}{1 + a_2(\Phi)hM \cdot f(M)} - \delta \right) M \quad (2)$$

$$\frac{dP_1}{dt} = \left(\varepsilon \frac{a_1(\Phi)M}{1 + a_1(\Phi)hM} - \delta \right) P_1 \quad (3)$$

$$\frac{dP_2}{dt} = \left(\varepsilon \frac{a_2(\Phi)M \cdot f(M)}{1 + a_2(\Phi)hM \cdot f(M)} - \delta \right) P_2 \quad (4)$$

The model describes a prey algal species M consuming nutrients N , and being consumed in turn by two predators P_1 and P_2 (Fig. 2). Nutrients, algae and predators are all measured in μmol nitrogen per liter. Nutrients flow into the system with dilution rate δ , and nutrients, prey and predators are washed out of the system at the same rate. N_0 is the nutrient concentration in the inflowing medium, r and K_M represent the maximum growth rate and half-saturation constant of the prey, and ε and h represent the predator's conversion efficiency and handling time. As algae take up only the amount of nitrogen that is converted into prey biomass we set the conversion efficiency of N into M to 1. We ignored natural predator mortality, because the dilution rate in algal-rotifer experimental systems is typically high compared to rotifer lifespan ($\delta = 0.55 \text{ d}^{-1}$, meaning the average time before being washed out is around 1.25 days, Table 1; the typical *Brachionus* lifespan is around 10 days (Weithoff and Wacker, 2007)).

The attack rates of the two predators, a_1 and a_2 , are functions of the prey edibility Φ , which may represent e.g. the size of the prey:

$$a_i(\Phi) = a_i^{(0)} \exp\left(-\frac{(\Phi_{i,0} - \Phi)^2}{s_i}\right) \quad (5)$$

This represents a Gaussian function with a maximum value $a_i^{(0)}$ at $\Phi = \Phi_{i,0}$, where the selectivity of the predators s_i determines the standard deviation. We assume one predator type is better at consuming prey with a low value of Φ , and the other can more easily consume prey with a high value of Φ , but the food spectra overlap (Fig. 3). The optimal value for predator 1 is $\Phi_{1,0}$ and for predator 2 $\Phi_{2,0}$, respectively.

Following the approach of quantitative genetics (Abrams, 2001), Φ changes along the fitness gradient (i.e. in the direction of higher prey fitness), with the speed of change determined by the slope of the gradient and by the additive genetic variance ν (Tirok et al., 2011; Lynch and Walsh, 1998; Wirtz, 2013):

$$\frac{d\Phi}{dt} = \nu \frac{\partial \left(\frac{1}{M} \frac{dM}{dt} \right)}{\partial \Phi} + \mu(\Phi) \quad (6)$$

$$\mu(\Phi) = c \left(\frac{1}{(b_l - \Phi)^2} - \frac{1}{(b_r - \Phi)^2} \right)$$

Within an individual simulation run, ν is kept constant in our model. To ensure that Φ stays within a range of biologically reasonable values, defined by the lower and upper boundaries b_l and b_r , we include the boundary function $\mu(\Phi)$ (see e.g. Abrams,

Table 1
Parameters used in the model described by Eqs. (1)–(6) and their values during simulations (Fussmann et al., 2000), with the exception of $a^{(0)}$ for which we chose a lower value than measured.

Variable	Value	Dimension	Biological interpretation
δ	0.55	d^{-1}	dilution rate
N_0	80	$\mu\text{mol N/l}$	nitrogen concentration in inflow
r	3.3	d^{-1}	maximal prey growth rate
K_M	4.3	$\mu\text{mol N/l}$	half saturation constant for prey growth
$a^{(0)}$	0.36	d^{-1}	maximal predator attack rate
h	0.11	$\text{d} \cdot \mu\text{mol N}$	handling time for predators
ε	0.25	–	predator conversion efficiency

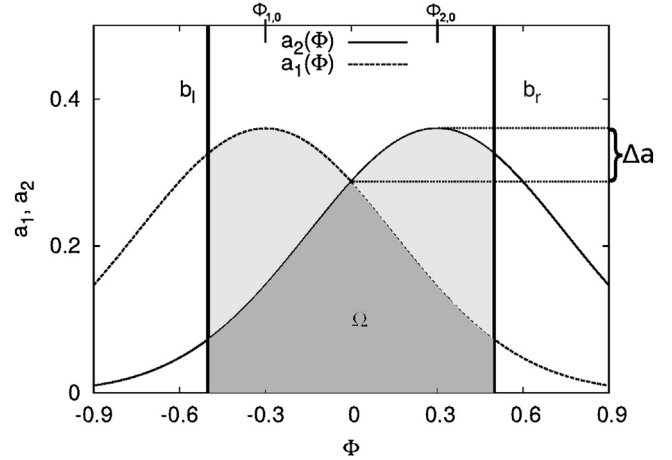


Fig. 3. Definition of two measures of predator similarity: the overlap in the prey spectrum $\Omega^{(rel)}$ and the maximum variation in attack rate Δa . The dark grey area is the absolute overlap Ω of $a_1(\Phi)$ and $a_2(\Phi)$ in the interval (b_l, b_r) marked by the vertical lines. Ω divided by all grey areas is the relative overlap $\Omega^{(rel)}$ in how the two predators exploit the prey spectrum. In this example, $s \approx 0.39$, resulting in $\Omega^{(rel)} = 0.5$ (see Eqs. (8)–(9)). Other parameters: $a^{(0)} = 0.36$, $\Phi_{1,0} = -0.3$, $\Phi_{2,0} = 0.3$, $b_l = -0.5$, $b_r = 0.5$.

2006, 2010; Klauschies et al., 2016). This could represent non-adaptive trait changes, e.g. mutation bias towards intermediate trait values, or stabilizing selection on the defence trait indicating that e.g. intermediate size is optimal for prey growth. We make no assumptions here on the mechanism for μ , but we assume its impact to be small ($c = 0.001$) in all simulations. In the absence of predators the trait value is pushed to $\Phi = \frac{b_l - b_r}{2} = 0$.

Finally, the model includes the possibility to simulate different feeding strategies of the two predators. With minor changes in the functional response of one predator type, the system can show very different kinds of dynamical behaviour for the two predators. The function $f(M)$ in Eqs. (2) and (4), for $M_0 > 0$, modifies the functional response of the second predator at very low densities of M :

$$f(M) = \frac{M}{M + M_0} \quad (7)$$

In this case grazing is reduced if the prey concentration is near the value of M_0 , which then stabilizes the system (Tirok et al., 2011). Such a functional response represents prey escaping predation at very low densities, e.g. due to small spatial heterogeneities, attachment to surfaces or cyst formation. Typically M_0 amounts to a very small fraction of the capacity (i.e. maximum prey abundance without predators, in this model represented by N_0). When $M_0 = 0$ (the standard simulation scenario), the functional responses of the two predators are identical ($f(M) = 1$), which is likely true for e.g. clones of *Brachionus*.

In general the parameters $a_i^{(0)}$, ε_i and s_i can be different for the two predator species. In this paper we assume that the two predators have the same values $a^{(0)}$, ε and s , and focus on differences in the parameter $\Phi_{i,0}$. The parameter values used were based on empirical data for an algae-rotifer system (Fussmann et al., 2000; Table 1).

2.2. Overlap in prey spectrum and variability of attack rates

The prey spectra of the predators $a_1(\Phi)$ and $a_2(\Phi)$ overlap, so that each predator can consume the prey even if the value of Φ is optimal for the other predator. We define the overlap of the two functions in the interval (b_l, b_r) of biologically meaningful values as

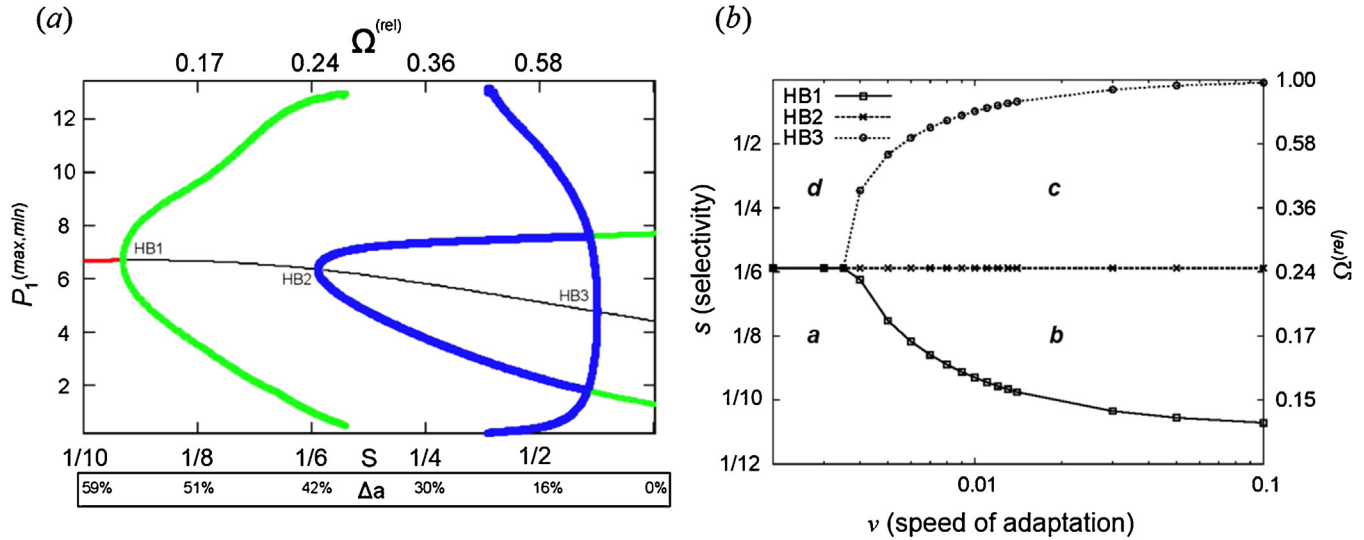


Fig. 4. Positions of Hopf bifurcations HB1, HB2 and HB3 delineating different oscillatory regimes. (a): speed of adaptation $v=0.01$; The red line indicates stable and the black line unstable stationary solutions. Green and blue lines represent the maximal and minimal biomass values of predator P_1 during the oscillations: green lines indicate stable oscillations (stable limit cycles) and blue lines indicate unstable limit cycles. In this range (s falling in between HB2 and HB3) the system oscillates between the two unstable limit cycles, resulting in complex oscillations (see dynamics shown in Fig. 5c). For intermediate predator selectivity s , the predators reach very low densities, and numerically go extinct. (b): Positions of the three Hopf bifurcations with varying v . Values are numerically calculated at the marked points. The axes for $\Omega^{(\text{rel})}$ and v are scaled logarithmically. The letters **a–d** indicate the regions in which the different oscillatory regimes shown in Fig. 5a–d occur. The faster the trait dynamics, the larger the parameter range between HB2 and HB3 where *predators taking turns* patterns are possible. (For interpretation of the references to colour in this figure legend, the reader is referred to the web version of this article.)

follows:

$$\Omega = \int_{b_l}^{b_r} \min(a_1(\Phi), a_2(\Phi)) d\Phi. \quad (8)$$

The relative overlap is then defined as

$$\Omega^{(\text{rel})} = \frac{\int_{b_l}^{b_r} \min(a_1(\Phi), a_2(\Phi)) d\Phi}{\int_{b_l}^{b_r} \max(a_1(\Phi), a_2(\Phi)) d\Phi}. \quad (9)$$

With this definition, $0 < \Omega^{(\text{rel})} \leq 1$. In case of $\Omega^{(\text{rel})} = 1$ the two functions $a_1(\Phi)$ and $a_2(\Phi)$ are identical in the interval (b_l, b_r) , while for $\Omega^{(\text{rel})} = 0$ there is no overlap. The former case is realised when $\Phi_{1,0} = \Phi_{2,0}$, or when $s = \infty$; the latter case is not possible in our model because the Gaussian curves are always greater than zero. In most simulations, a relative overlap of $\Omega^{(\text{rel})} \approx 0.5$ was used. We defined the left boundary b_l to be smaller than $\Phi_{1,0}$, and analogously b_r was defined to be larger than $\Phi_{2,0}$. Because our interest is in a scenario where minor trait changes may affect the dynamics, we restricted the interval (b_l, b_r) to extend only slightly beyond $\Phi_{1,0}$ and $\Phi_{2,0}$: $b_l = \Phi_{1,0} - 0.2$ and $b_r = \Phi_{2,0} + 0.2$, respectively.

Another measure of the difference between the two predator types is the possible variability in the attack rates Δa (see Fig. 3). The maximal value of both a_1 and a_2 is $a^{(0)}$ (see Eq. (5)). If Φ oscillates between b_l and b_r the minimal value of $a_i(\Phi)$ will be $a_i(0)$, as long as $2 \cdot \Phi_{1,0} < b_l < \Phi_{1,0}$ and $\Phi_{2,0} < b_r < 2 \Phi_{2,0}$. So the relative variation of a_i is calculated as follows:

$$\Delta a = \frac{a^{(0)} - a_i(0)}{a^{(0)}} = 1 - \exp\left(-\frac{\Phi_{i,0}^2}{s}\right) \quad (10)$$

In our model we chose a symmetric setup with $\Phi_{1,0} = -0.3$ and $\Phi_{2,0} = 0.3$, so that there is no difference in Δa for the two predators.

2.3. Numerical methods

For our numerical simulations we solved system (1)–(7) with a fourth order Runge–Kutta integration scheme implemented in Fortran. As initial conditions for the simulations we used $N(0) = 10 \mu\text{mol N/l}$; $M(0) = 10 \mu\text{mol N/l}$; $P_1(0) = 10 \mu\text{mol N/l}$ and $P_2(0) = 5 \mu\text{mol N/l}$; we used asymmetric initial conditions for the two predators to prevent the system from remaining stuck at the (always present but often unstable) equilibrium with $P_1 = P_2$. The first 300 days of the simulation are considered transient dynamics, and are ignored in all figures shown. Bifurcation diagrams are computed with help of the free bifurcation analysis software tool XPPAUT² and validated with our own numerical simulations.

3. Results

Two parameters are the most relevant for the analysis of this model: the selectivity s of the predators, which has a direct effect on the overlap in the prey spectrum $\Omega^{(\text{rel})}$; and the speed of adaptation v , which defines the relative timescales of evolutionary and ecological changes.

Fig. 4a shows the possible solutions of the model for varying selectivity s (and thus varying $\Omega^{(\text{rel})}$). The total range of s is divided into different dynamical regimes by three Hopf bifurcations: one ecological bifurcation (HB2) and two evolutionary bifurcations (HB1 and HB3). The ecological bifurcation HB2 is the point where, if no prey adaptation is taking place (i.e. prey defence remains constant at $\Phi = 0$), the system switches from stable predator-prey coexistence to predator-prey cycles. When s is low (i.e. the predators are distinct), the predator attack rates $a_i^{(0)}$ at $\Phi = 0$ are low, resulting in a stable equilibrium. Conversely, when s is high, the resulting high attack rates give rise to classic 1/4-lag predator-prey cycles.

A second type of cycling is found in the range between the evolutionary bifurcations HB1 and HB3: relatively slow cycles with

² <http://www.math.pitt.edu/~bard/xpp/xpp.html>.

ongoing trait changes on both trophic levels, driven by a co-evolutionary arms race between prey and predators. These cycles are not possible if s is either very low or very high. If s is larger than HB3, the prey spectra of the two predators are nearly identical, and selective pressure on prey defence is too weak to cause deviations from $\Phi=0$ (the stabilizing effect of μ becomes the stronger pressure). On the other extreme, if s is smaller than HB1, the prey gains a strong advantage from staying in the middle ($\Phi=0$) because this strongly reduces the attack rates of both predators. In both cases the optimal defence strategy for the prey is always $\Phi=0$, and neither predator can gain an advantage over the other and dominate the system. However, if s falls between HB1 and HB3, the two predators oscillate in antiphase with each other, causing recurrent reversals in selection on prey defence Φ . As one of the predators becomes dominant, selective pressure causes Φ to change in favour of the other predator, allowing it to recover and become the new dominant predator. This reverses selective pressure on Φ , leading to repeated alternations in the dominance of the two predator types, preventing either of them from going extinct.

Thus, the three bifurcation points HB1, HB2 and HB3 divide the total range of s into four oscillatory regimes, each characterized by a combination of presence or absence of ecological and evolutionary cycles. For very low s (very little overlap in prey spectra between the predators), neither ecological nor evolutionary cycles occur, and the system converges to a stationary state (Fig. 5a). Conversely, for very high s , prey defence remains constant at $\Phi=0$ and only ecological cycles occur. This results in regular 1/4-lag predator-prey cycles where the densities of the two predators are equal, and the predators oscillate in synchrony (Fig. 5d). When s

falls between HB1 and HB2, only evolutionary cycles occur: the predators cycle in antiphase with each other, and the total predator density remains relatively constant (Fig. 5b). Finally, when s falls between HB2 and HB3, both the slow evolutionary cycles and the rapid 1/4-lag predator-prey cycles are present, resulting in complex oscillations with variable amplitudes (Fig. 5c).

The range between HB2 and HB3 is the oscillatory regime in which intermittent cycles are possible. The width of this range is determined by the distance between these two Hopf bifurcations, which may depend on different parameters; the parameter most strongly affecting this is the speed of adaptation ν (Fig. 4b). The position of the ecological bifurcation HB2 is independent of ν ; in contrast, the positions of both HB1 and HB3 are strongly dependent on ν , moving farther apart as adaptation becomes more rapid (Fig. 4b). For fast adaptation, even predators with almost identical prey spectrum ($\Omega^{(rel)} \approx 1$) can alternate their dominance, resulting in a *predators taking turns* pattern. Conversely, as the speed of prey adaptation becomes very slow, the positions of HB1 and HB3 converge towards the ecological Hopf bifurcation HB2. After the collision of HB1 and HB2, the only possible system dynamics are a stable equilibrium (low s) and regular predator-prey cycles (high s). At this point there is no evolution in either prey or predator, and the system is identical to the classical case with a single predator and a single prey species.

Other parameters may affect the probability of finding intermittent cycles by changing the position of HB2. Increasing the maximum attack rate $a^{(0)}$ shifts HB2 to the left (Appendix A, Fig. A1), strongly increasing the range of s for which intermittent cycles can be found, and the same is true for decreasing the prey growth rate r (Fig. A2). The handling time h and half-saturation

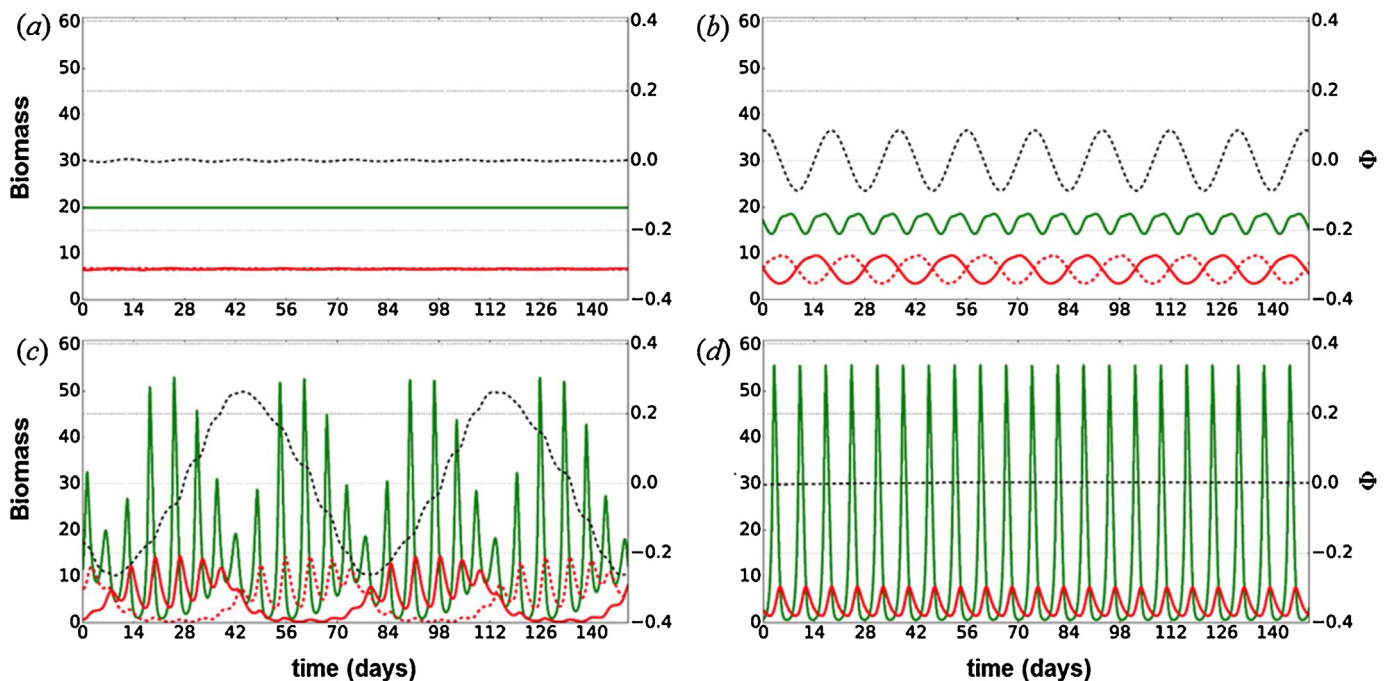


Fig. 5. Different dynamical solutions for different values of selectivity s . All panels show prey M (green lines), predators P_1 and P_2 (solid and dashed red lines), and the trait value Φ (dashed black line). $\nu = 0.01$ (slow prey adaptation) in all cases. Biomasses are given in $\mu\text{mol N/l}$. (a): $s = 0.1$ ($\Omega^{(rel)} \approx 0.12$, $\Delta a \approx 59\%$). The two predators are specialists, enabling prey to avoid predation by remaining at $\Phi \approx 0$. (b): $s = 0.125$ ($\Omega^{(rel)} \approx 0.17$, $\Delta a \approx 51\%$). Minor deviations from panel (a) result in oscillations of Φ with *predators taking turns* patterns. The oscillations of Φ result in an oscillatory attack rate for each predator between $a_{\min} \approx 0.18 \text{ d}^{-1}$ and $a_{\max} \approx 0.36 \text{ d}^{-1}$. (c): $s = 0.4$ ($\Omega^{(rel)} \approx 0.51$, $\Delta a \approx 20\%$). *Predators taking turns* patterns lead to variations in the amplitudes of the oscillation. The oscillations of Φ result in an oscillatory attack rate for each predator between $a_{\min} \approx 0.29 \text{ d}^{-1}$ and $a_{\max} \approx 0.36 \text{ d}^{-1}$. (d): $s = 2.0$ ($\Omega^{(rel)} \approx 0.86$, $\Delta a \approx 4\%$). The differences between the two predators are too small to show *predators taking turns* patterns; $\Phi \approx 0$. Note that in (a) and (d) the prey is equally well defended against both predators, and the biomasses of P_1 and P_2 overlap. (For interpretation of the references to colour in this figure legend, the reader is referred to the web version of this article.)

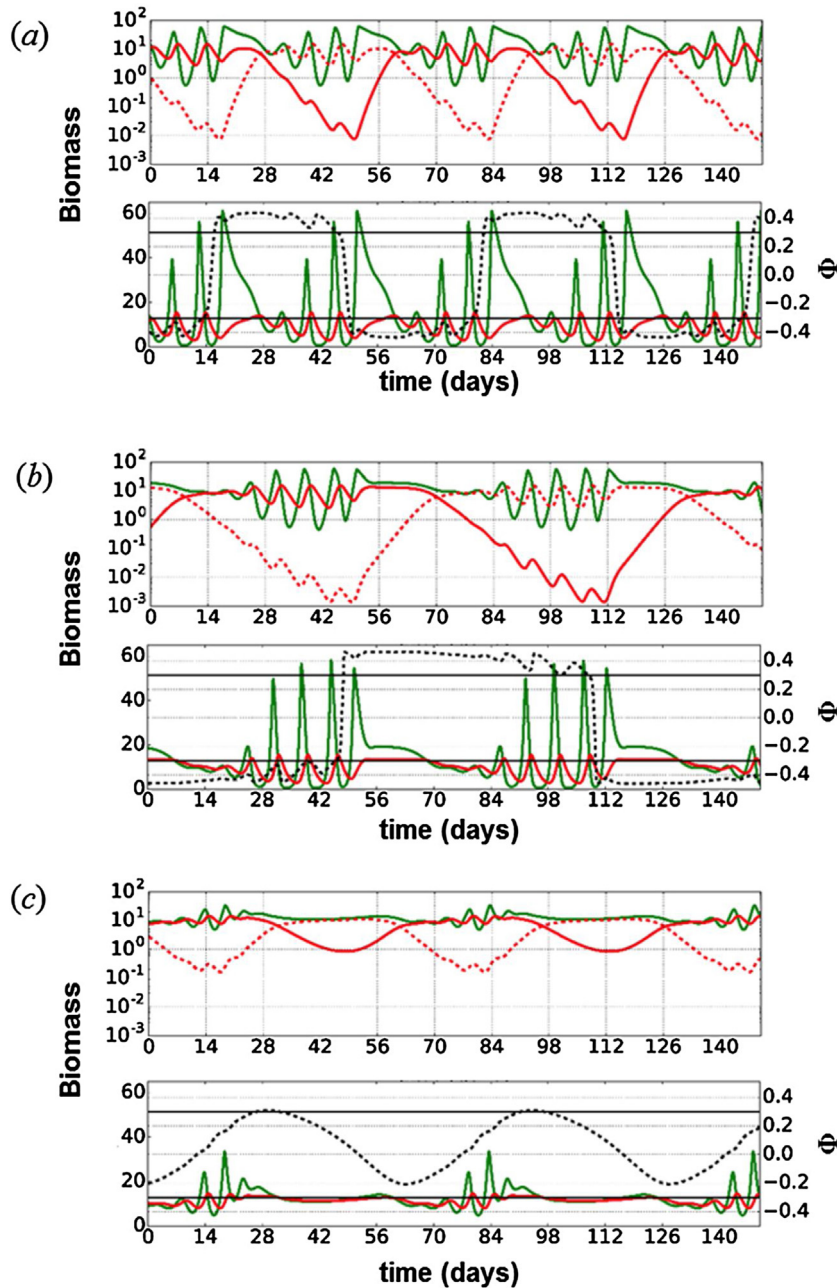


Fig. 6. Intermittent cycles driven by (a–b) rapid prey adaptation and (c) slight differences in the functional responses of the predators. Top panels show the population densities of prey M (green line) and predators P_1 and P_2 (red solid and dashed line); bottom panels show population densities of prey M (green line) and the sum of the two predators (red line), as well as the trait value Φ (dashed black line). The two horizontal lines in the bottom panels indicate the optimal trait values for the two predators $\Phi_{(1,0)}$ and $\Phi_{(2,0)}$. (a–b): Predators taking turns patterns with a relatively high speed of trait adaptation ν leads to sudden trait shifts and more complex dynamics than those shown in Fig. 5c. (a) $\nu=0.1$, $s=0.4$ ($\Omega^{(rel)} \approx 0.51$, $\Delta a \approx 20\%$); (b) $\nu=0.1$, $s=0.67$ ($\Omega^{(rel)} \approx 0.66$, $\Delta a \approx 13\%$). (c): Different functional responses can cause different alternating solution depending on which predator is dominant (stationary and oscillatory). $\nu=0.01$, $M_0=3$, $s=0.4$ ($\Omega^{(rel)} \approx 0.51$, $\Delta a \approx 20\%$). (For interpretation of the references to colour in this figure legend, the reader is referred to the web version of this article.)

constant K_M did not have any substantial impact on the likelihood of intermittent cycles (Figs. A3 and A4).

3.1. Complex oscillations in predators taking turns patterns

We now take a closer look at the *predators taking turns* patterns between HB2 and HB3 (Fig. 5c). The simulation shown in Fig. 6a was performed with the same parameter values, except with faster prey adaptation ($\nu=0.1$). In this case, the prey trait Φ can potentially change faster than the biomasses of the predator species. This results in sudden shifts of the trait variable Φ . The

predator-prey oscillations are interrupted during the period when the previously dominant predator declines and the other emerges. For this speed of prey evolution, this intermittent pattern can be seen even when the difference between the two predator types is quite small ($\Omega^{(rel)} \approx 0.66$, $\Delta a \approx 13\%$; Fig. 6b).

Because the shift in Φ occurs more rapidly than the emergence of the new dominant predator, the trait value exceeds the value $\Phi_{(1,0)}$ (or $\Phi_{(2,0)}$, respectively) and then remains relatively constant. This provides enough time for the dominant predator to develop oscillations with the prey with increasing amplitude. These oscillations, combined with the boundary function $\mu(\Phi)$, finally

cause the prey trait Φ to cross the value $\Phi_{(1,0)}$ (or $\Phi_{(2,0)}$) again in the other direction. As a result, the prey quickly becomes defended against the dominant predator, and the same pattern starts for the other predator.

If one predator has a sigmoid functional response for low prey abundance (see Eq. (7)), rather than a type II, this can lead to an almost stationary dynamic between this predator and the prey. In the range between HB2 and HB3, where there are 1/4-lag cycles between the prey and the other predator, this can then lead to alternating oscillatory and stationary dynamics between the prey and the sum of the two predators (Fig. 6c). It is necessary for this dynamical solution that the predator with a sigmoid functional response reaches very low densities during the dominance of the other predator to enable it to oscillate with the prey density. If both predators have a sigmoid functional response, 1/4-lag oscillations (i.e. ecological cycles) are not possible at all, and the ecological bifurcation HB2 disappears. In this case, only evolutionary cycles can be found between HB1 and HB3, and intermittent cycles are not possible.

4. Discussion

Contemporary evolution in predator-prey systems can leave distinct signatures in the characteristics of predator-prey cycles, allowing us to deduce afterwards that evolution must have been present in the system. As the most famous example, antiphase cycles are considered to be a “smoking gun” for the presence of rapid prey evolution (Yoshida et al., 2003; Becks et al., 2010; Jones and Ellner, 2007). Re-evaluating data from old experiments indicated that such rapid evolution had taken place in many experiments exhibiting antiphase cycles (Hiltunen et al., 2014b). A similar approach has been used for detecting the presence of prey evolution in two-predator systems with intraguild predation (Hiltunen et al., 2014a). Our results suggest that intermittent cycles, where regular 1/4-lag predator-prey cycles are briefly interrupted before re-asserting themselves (Fig. 1), may be a signature for the presence of ongoing predator-prey co-adaptation. This conclusion is in line with previous work showing that adaptation in both prey and predators can cause variations in amplitudes of predator-prey cycles (Mougi and Nishimura, 2007; Mougi, 2012) and interruptions of the 1/4-lag pattern (Abrams and Shen, 1989; Tirok et al., 2011). However, in these models the potential for adaptation was large, which does not reflect chemostat experiments with one predator and one prey type.

While some amount of trait variation is always present among living organisms even without age-structure or substantial genetic variation, it is much less than e.g. the large differences in prey edibility that are required for antiphase cycles (Becks et al., 2010; Jones and Ellner, 2007).

Hence, our aim was to discover what degree of variation in the predators, and adaptation in the prey, would be necessary to produce intermittent cycles. Strikingly, our results indicate that the degree of adaptation necessary to produce intermittent cycles is rather minimal: depending on the speed of adaptation in the prey, we may see this dynamic behaviour already when predator attack rates show around 10% variation. This degree of trait variation, while substantial enough to cause striking deviations in predator-prey dynamics, is small enough to fall within the large measurement errors usually found for such traits (e.g. Seifert et al., 2014), and thus may go unnoticed in experimental systems.

In contrast with the signature left by prey adaptation alone, where strong trait oscillations take place over the same period as a single predator-prey cycle (Becks et al., 2010; Jones and Ellner, 2007), intermittent cycles are an indication that adaptation is slower than the ecological dynamics. The interruptions of the 1/4-lag are caused by the shift in the prey trait and the condition for generating intermittent dynamics is that several regular 1/4-lag cycles pass in between two trait shifts. This means that there must be a time lag between the emergence of the new dominant predator and the prey’s adaptive response to it, allowing the dominant predator to develop 1/4-lag cycles with the prey. In our model, this time lag in adaptation is generated either by slow adaptation in the prey, or by the prey trait overshooting its optimum. However, other possible mechanisms can be imagined as well: for example, if the trait shift is rapid and strong enough that the disfavoured genotype(s) becomes extremely rare, it may take many generations before any notable degree of defence can re-establish in the population.

In effect, intermittent cycles are the result of combining two simultaneous, superimposed oscillations: the “ecological” 1/4-lag cycles and a slower “evolutionary” trait cycle. This results in temporal variation in attack rates, and through this, variability in the amplitudes of the predator-prey oscillations. Various minor changes to the model, such as rapid prey adaptation or slight differences in predator functional responses, can then give rise to even more complex patterns (Fig. 6). Additionally, even if 1/4-lag oscillations are only dampened rather than completely interrupted, this may look indistinguishable from intermittent cycles in

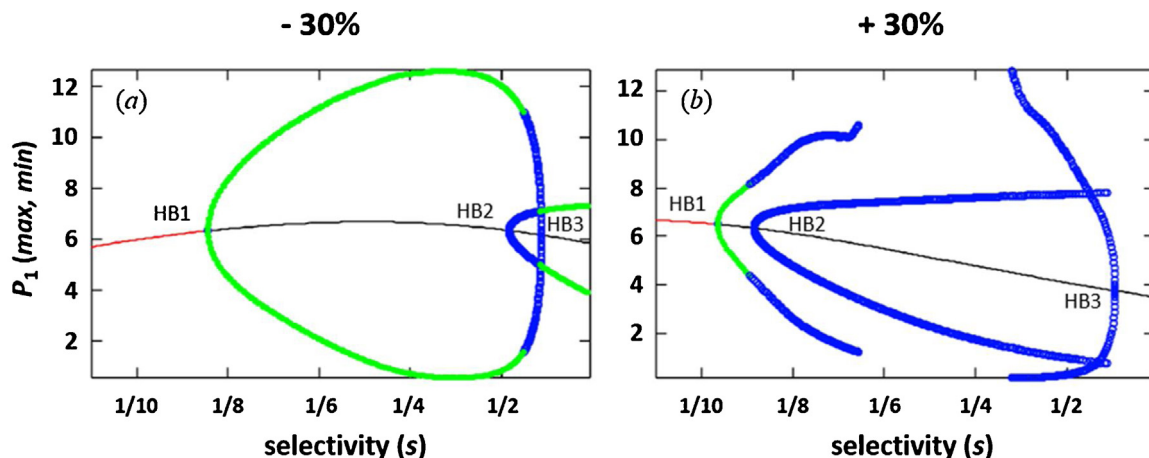


Fig. A1. Positions of Hopf bifurcations HB1, HB2 and HB3 delineating different oscillatory regimes for (a) a lower maximum attack rate, $a^{(0)}=0.25$ and (b) higher maximum attack rate, $a^{(0)}=0.47$. All other parameters the same as in Table 1 and Fig. 4. The red line indicates stable, and the black line unstable stationary solutions. Green and blue lines represent the maximal and minimal biomass values of predator P_1 during the oscillations: green lines indicate stable oscillations (stable limit cycles) and blue lines indicate unstable limit cycles. (For interpretation of the references to colour in this figure legend, the reader is referred to the web version of this article.)

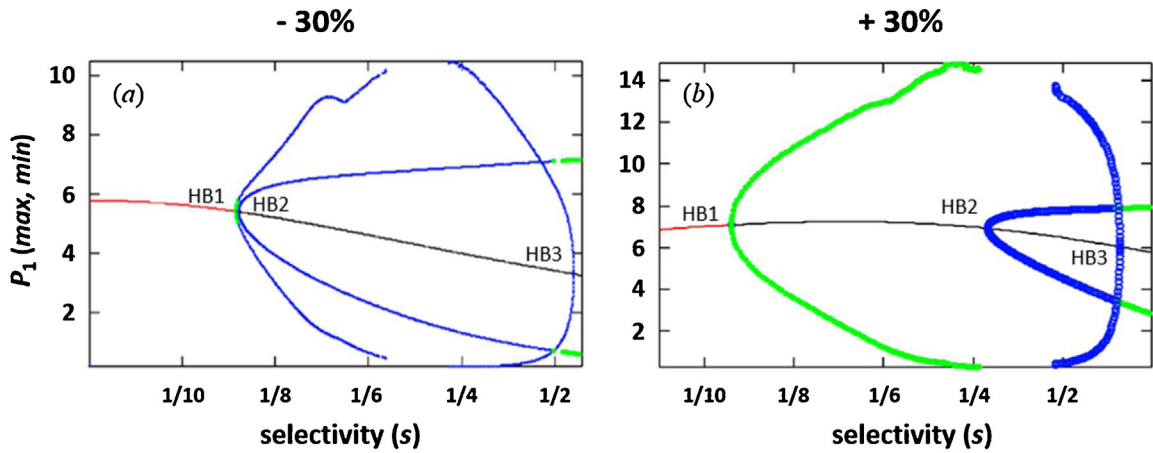


Fig. A2. Positions of Hopf bifurcations HB1, HB2 and HB3 delineating different oscillatory regimes for (a) a lower prey growth rate, $r=2.31$ and (b) higher prey growth rate, $r=4.29$. All other parameters the same as in Table 1 and Fig. 4. Colours have the same meaning as in Fig. A1. In (a), a smaller point size was used to avoid overlap between the bifurcation points HB1 and HB2.

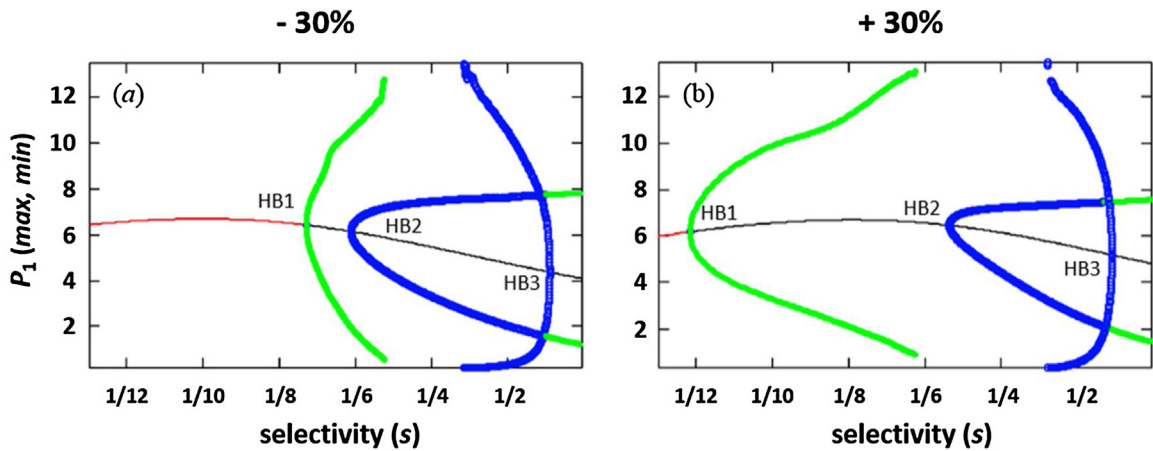


Fig. A3. Positions of Hopf bifurcations HB1, HB2 and HB3 delineating different oscillatory regimes for (a) a shorter handling time, $h=0.077$; and (b) longer handling time, $h=0.143$. All other parameters the same as in Table 1 and Fig. 4. Colours have the same meaning as in Fig. A1.

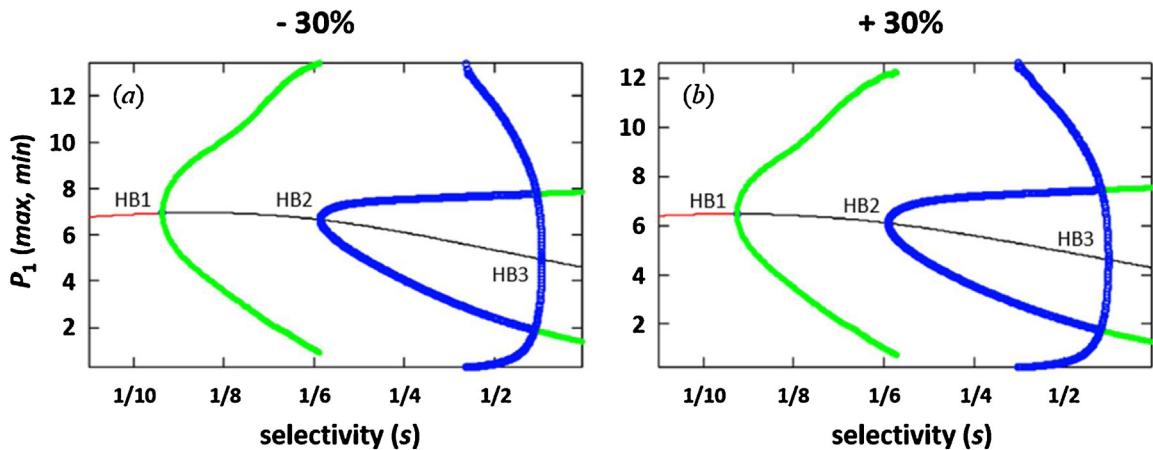


Fig. A4. Positions of Hopf bifurcations HB1, HB2 and HB3 delineating different oscillatory regimes for (a) a lower half-saturation constant, $K_M=3.01$; and (b) higher half-saturation constant, $K_M=5.59$. All other parameters the same as in Table 1 and Fig. 4. Colours have the same meaning as in Fig. A1.

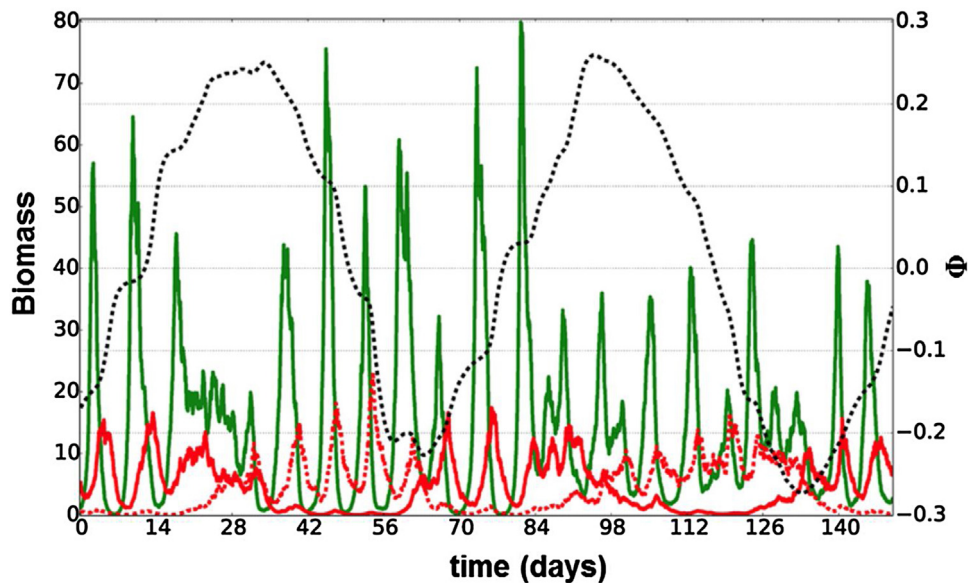


Fig. B1. The phase difference between oscillations with small amplitudes is not obvious if multiplicative noise is considered in the system. Parameters and conditions are the same as in Fig. 5c. The Eqs. (1)–(4) have an additional term $+\omega X(t)\xi(t)$, where $X(t)$ denotes the system component (N , M , P_1 or P_2 , respectively) and $\xi(t)$ is a Gaussian distributed random number with mean 0 and variance equal to 1, assuming no covariance between $\xi(t)$ at successive time points (i.e. white noise). The noise-intensity in this example is $\omega=0.2$.

an empirical time series. For example, if we add small amounts of noise to the system, small amplitude oscillations might be interpreted as stationary solutions, or antiphase oscillations (see Appendix B).

A very different mechanism for intermittent cycles was studied by Yamamichi et al. (2011): temporal switching between the dominance of phenotypically plastic prey (promoting stability in dynamics) and non-plastic prey (promoting predator-prey cycles). Because stability favours non-plastic prey and oscillations favour plastic prey, this causes a complex feedback loop resulting in alternation between stable and oscillatory dynamics. As far as we are aware, this is the only mechanism that may intrinsically generate intermittent cycles without requiring trait variation or adaptation in the predator. It should be noted that this study assumes very large differences in edibility between prey phenotypes, and it is unclear whether its results would hold up under the much smaller differences we have studied.

Our model shows that minor variations from a single-predator single-prey system can leave a major imprint on the dynamical behaviour of the system. Because chemostat experiments in which regular 1/4-lag cycles broke down or stabilized on a stationary state were often terminated in the past (e.g. Gause et al., 1936; Huffaker, 1958; Luckinbill, 1974; Ellner et al., 2001), it is impossible to say whether regular 1/4-lag cycles could have re-asserted themselves if the experiments had been allowed to continue, thus turning into intermittent cycles. The fact that such intermittent cycles were observed in long-term chemostat data suggests this is a possibility, and it is likely that intermittent cycles are under-reported in published studies.

Because we explicitly looked for effects of trait variation that may go undetected, it is difficult to give evidence that such processes are indeed taking place in existing chemostat data, including the dynamics shown in Fig. 1. Recent laboratory experiments indicate that rotifer clones of the same species, similar in appearance, might differ in the efficiency to use the same prey species *Nannochloropsis limnetica* (S. Schälicke and A. Wacker, pers. comm.). Thus, testing the effects of minor clonal variation on predator-prey dynamics experimentally may provide a new

avenue for further research and towards understanding complex predator-prey dynamics.

Acknowledgements

The authors thank Guntram Weithoff for the chemostat data, and Bernd Blasius, Elias Ehrlich, Toni Klauschies, Horst Malchow, Michael Raatz and Guntram Weithoff for helpful discussions and ideas. Furthermore, we cordially thank two anonymous reviewers whose revealing comments on our manuscript helped to improve the presentation of our results. This research was funded by the Deutsche Forschungsgemeinschaft (DFG) within the Priority Programme 1704 Flexibility matters: Interplay between trait diversity and ecological dynamics using aquatic communities as model systems (DynaTrait) (MA1451/12-1 and GA401/26-1).

Appendix A. Sensitivity analysis

Because of the inherent and sometimes substantial uncertainty in measuring the system parameters in chemostat systems, we tested the sensitivity of our results to the specific parameter values used. For this we performed the bifurcation analysis shown in Fig. 4a with each parameter decreased or increased by 30%. Because the prey-predator conversion efficiency ε merely scales the ratio of predator and prey biomass and is unlikely to impact the dynamics, we did not include this parameter in the sensitivity analysis. We also excluded the dilution rate δ or the nutrient concentration N_0 , as these parameters are set by the experiment and thus accurately known.

Appendix B. Noisy predators taking turn patterns

Usually we do not know about all factors determining the ecological processes in an experimental system. Some factors might be sensitive against small variations in, for example, temperature and light condition. These unknown factors can be modelled as random disturbances in the system components

which are proportional to their current values. Depending on the strength of such multiplicative noise, the phase difference during predator-prey oscillations with small amplitudes might not be as clear as in the deterministic case. An example of this is shown in Fig. B1, which displays a result from a simulation using the same set of parameters as used in Fig. 5c, but with multiplicative noise for all system components.

References

- Abrams, P.A., Shen, L., 1989. Population dynamics of systems with consumers that maintain a constant ratio of intake rates of two resources. *Theor. Popul. Biol.* 35, 51–89.
- Abrams, P.A., 2000. The evolution of predator-prey interactions: theory and evidence. *Annu. Rev. Ecol. Syst.* 31, 79–105.
- Abrams, P.A., 2001. Modelling the adaptive dynamics of traits involved in inter- and intraspecific interactions: An assessment of three methods. *Ecol. Lett.* 4, 166–175.
- Abrams, P.A., 2006. The prerequisites for and likelihood of generalist-specialist coexistence. *Am. Nat.* 167, 329–342.
- Abrams, P.A., 2010. Quantitative descriptions of resource choice in ecological models. *Popul. Ecol.* 52, 47–58.
- Becks, L., Ellner, S.P., Jones, L.E., Hairston Jr., N.G., 2010. Reduction of adaptive genetic diversity radically alters eco-evolutionary community dynamics. *Ecol. Lett.* 13, 989–997.
- Bulmer, M.G., 1976. The theory of prey-predator oscillations. *Theor. Popul. Biol.* 9, 137–150.
- Ellner, S.P., Becks, L., 2011. Rapid prey evolution and the dynamics of two-predator food webs. *Theor. Ecol.* 4, 133–152.
- Ellner, S.P., McCauley, E., Kendall, B.E., et al., 2001. Habitat structure and population persistence in an experimental community. *Nature* 412, 538–543.
- Elton, C., Nicholson, M., 1942. The ten-year cycle in numbers of the lynx in Canada. *J. Anim. Ecol.* 11, 215–244.
- Fussmann, G.F., Ellner, S.P., Shertzer, K.W., Hairston Jr., N.G., 2000. Crossing the Hopf bifurcation in a live predator-prey system. *Science* 290, 1358–1360.
- Fussmann, G.F., Ellner, S.P., Hairston Jr., N.G., 2003. Evolution as a critical component of plankton dynamics. *Proc. R. Soc. B* 270, 1015–1022.
- Fussmann, G.F., Ellner, S.P., Hairston Jr., N.G., Jones, L.E., Shertzer, K.W., Yoshida, T., 2005. Ecological and evolutionary dynamics of experimental plankton communities. *Adv. Ecol. Res.* 37, 221–243.
- Gause, G.F., Smaragdova, N.P., Witt, A.A., 1936. Further studies of interaction between predators and prey. *J. Anim. Ecol.* 5, 1–18.
- Gilg, O., Hanski, I., Sittler, B., 2003. Cyclic dynamics in a simple vertebrate predator-prey community. *Science* 302, 866–868.
- Hiltunen, T., Ellner, S.P., Hooker, G., Jones, L.E., Hairston Jr., N.G., 2014a. Eco-evolutionary dynamics in a three-species food web with intraguild predation: intriguingly complex. *Adv. Ecol. Res.* 50, 41–73.
- Hiltunen, T., Hairston Jr., N.G., Hooker, G., Jones, L.E., Ellner, S.P., 2014b. A newly discovered role of evolution in previously published consumer-resource dynamics. *Ecol. Lett.* 17, 915–923.
- Huffaker, C.B., 1958. Experimental studies on predation: dispersion factors and predator-prey oscillations. *Hilgardia* 27, 343–383.
- Jones, L.E., Ellner, S.P., 2007. Effects of rapid prey evolution on predator-prey cycles. *J. Math. Biol.* 55, 541–573.
- Klauschies, T., Vasseur, D.A., Gaedke, U., 2016. Trait adaptation promotes species coexistence in diverse predator and prey communities. *Ecol. Evol.* 6, 4141–4159.
- Lotka, A.J., 1925. *Elements of Physical Biology*. Williams & Wilkins Company.
- Luckinbill, L.S., 1974. The effects of space and enrichment on a predator-prey system. *Ecology* 55, 1142–1147.
- Lynch, M., Walsh, B., 1998. *Genetics and Analysis of Quantitative Traits*. Sinauer, Sunderland, MA.
- McCauley, E., Nisbet, R.M., Murdoch, W.W., de Roos, A.M., Gurney, W.S.C., 1999. Large-amplitude cycles of *Daphnia* and its algal prey in enriched environments. *Nature* 402, 653–656.
- Mougi, A., Nishimura, K., 2007. A resolution of the paradox of enrichment. *J. Theor. Biol.* 248, 194–201.
- Mougi, A., 2012. Unusual predator-prey dynamics under reciprocal phenotypic plasticity. *J. Theor. Biol.* 305, 96–102.
- Rosenzweig, M.L., MacArthur, R.H., 1963. Graphical representation and stability conditions of predator-prey interactions. *Am. Nat.* 97, 209–223.
- Seifert, L.I., de Castro, F., Marquart, A., Gaedke, U., Weithoff, G., Vos, M., 2014. Heated relations: temperature-mediated shifts in consumption across trophic levels. *PLoS One* 9, e95046.
- Tirok, K., Bauer, B., Wirtz, K., Gaedke, U., 2011. Predator-prey dynamics driven by feedback between functionally diverse trophic levels. *PLoS One* 6, e27357.
- Truscott, J.E., Brindley, J., 1994. Ocean plankton populations as excitable media. *Bull. Math. Biol.* 56, 981–998.
- Utida, S., 1957. Cyclic fluctuations of population density intrinsic to the host-parasite system. *Ecology* 38, 442–449.
- Volterra, V., 1928. Variations and fluctuations of the number of individuals in animal species living together. *J. Cons. Int. Explor. Mer.* 3, 3–51.
- Weithoff, G., Wacker, A., 2007. The mode of nutrition of mixotrophic flagellates determines the food quality for their consumers. *Funct. Ecol.* 21, 1092–1098.
- Wirtz, K.W., 2013. Mechanistic origins of variability in phytoplankton dynamics: part I: niche formation revealed by a size-based model. *Mar. Biol.* 160, 2319–2335.
- Yamamichi, M., Yoshida, T., Sasaki, A., 2011. Comparing the effects of rapid evolution and phenotypic plasticity on predator-prey dynamics. *Am. Nat.* 178, 287–304.
- Yoshida, T., Jones, L.E., Ellner, S.P., Fussmann, G.F., Hairston Jr., N.G., 2003. Rapid evolution drives ecological dynamics in a predator-prey system. *Nature* 424, 303–306.